INVENTORY OF SUPPLEMENTAL INFORMATION

Figure S1, related to Figure 1.

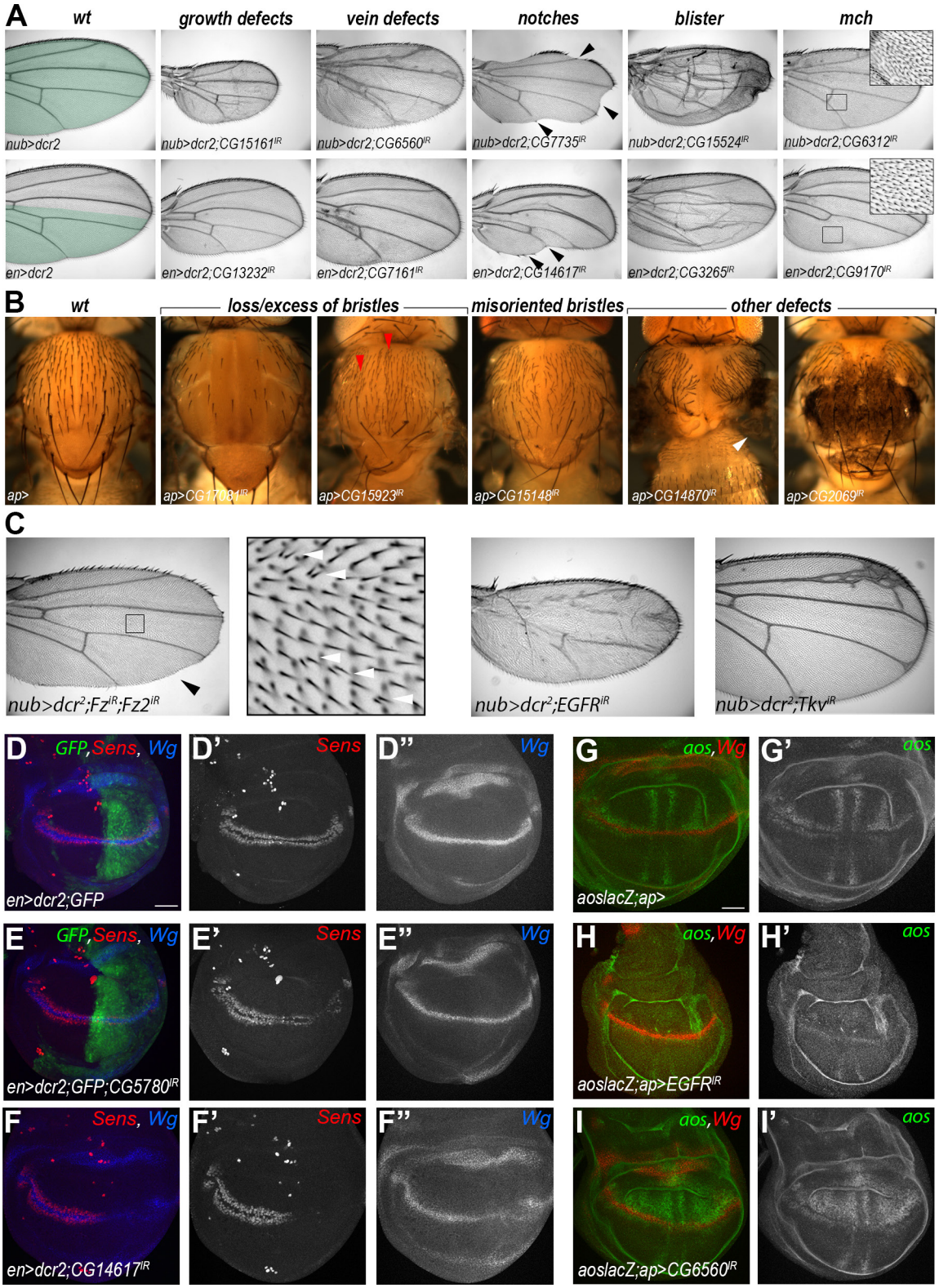

Phenotypes observed during primary and secondary screening.

(**A-B**) Examples of phenotypes of the primary screen: adult wings are oriented proximal to the left and anterior up; thorax orientation is anterior up.

(**A**) Examples of phenotypes observed in each category in the wing using *nubGal4* (*nub>*, expressed in the entire wing, domain highlighted in green in upper left panel) and *enGal4* (*en>*, expressed in the posterior compartment, highlighted in green in lower left panel), black arrowheads point toward notches; high magnification inserts in right most panels show examples of multiple cellular hair (mch) phenotypes (indicated by black square in full wing view). (**B**) Examples of phenotypes observed for each category in the thorax using *apGal4* (*ap>*, expressed in the entire notum).

(**C**) Phenotypes induced by knockdown of components of the different developmental signaling pathways using *nub>*, black arrowheads point toward notches, square in *fz*/*fz2* KD panel indicates area shown at high magnification next to the image displaying mch phenotypes (white arrowhead).

(**D-I**) Examples of phenotypes observed in the secondary screen, wing discs are oriented anterior left and dorsal up. (**D**) Wt patterns of Sens (red, monochrome in **D'**) and Wg (blue, monochrome in **D"**), used as markers for activation of canonical Wg and Notch pathways, respectively, in flies expressing GFP under the control of *en>*. (**E-F**) Examples of CG5780-IR leading to disruption of Sens expression only (**E**), and CG14617-IR disrupting both Wg and Sens induction (**F**). (**G**) Wt pattern of the EGFR signaling as reported by *aos-lacZ* (green, monochrome in **G'**) in flies expressing *apGal4*, Wg staining (red) is used to delimit the dorsal compartment (where *ap>* is expressed) and the wt ventral compartment. (**H**) Loss of EGFR via RNAi leads to loss of *aos-lacZ* expression in the dorsal compartment. (**I**) Example of RNAi against CG6560 causing an increase in *aos-lacZ* expression in our secondary screen. Scale bars in (**D, G**) represent 25μm.

Figure S2, related to Figure 2

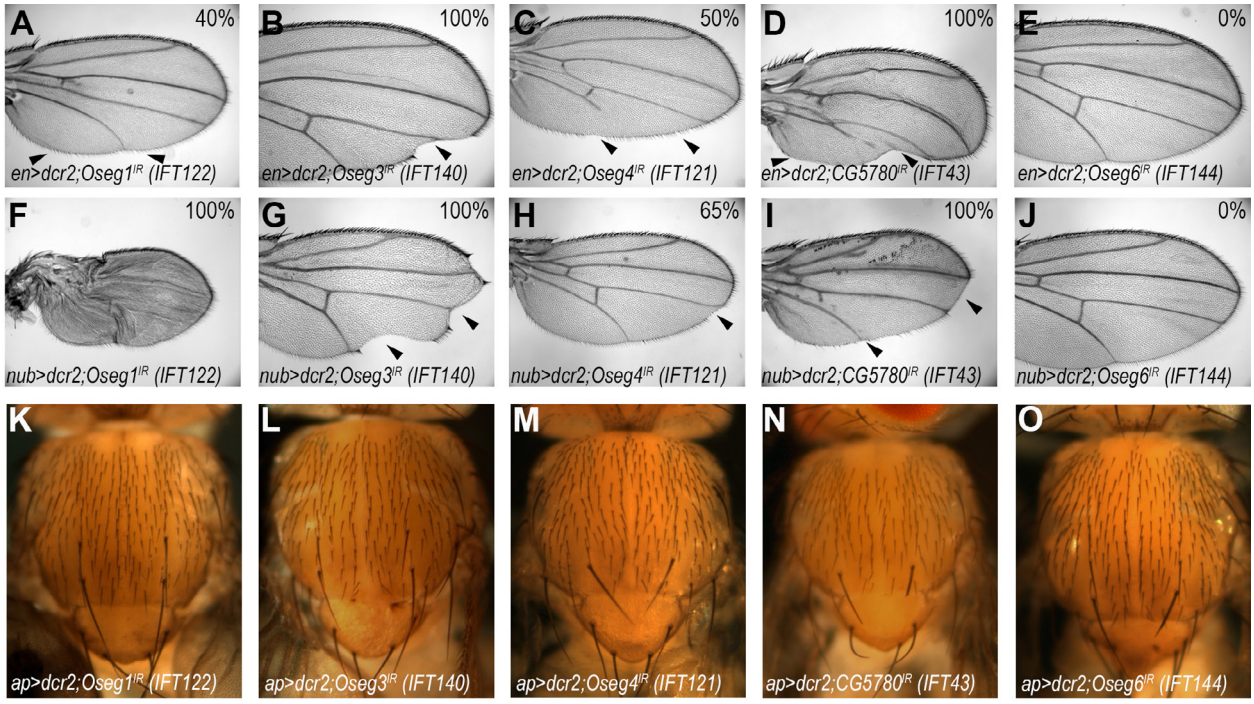

P

		CONTROLS			IFT-A KD				
HEDGEHOG PATHWAY		**w1118**	**Smo-IR**	**Ptc-IR**	**IFT121-IR**	**IFT122-IR**	**IFT140-IR**	**IFT43-IR**	**IFT144-IR**
ap>GFP	Ptc staining	no effect	downregulation	downregulation	no effect	no effect	no effect	no effect	no effect
	Ci Staining	no effect	downregulation	upregulation	no effect	no effect	no effect	no effect	no effect
NOTCH PATHWAY		**w1118**	**Notch-IR**		**IFT121-IR**	**IFT122-IR**	**IFT140-IR**	**IFT43-IR**	**IFT144-IR**
en>dcr2	Wg staining	no effect	downregulation		no effect	no effect	no effect	no effect	no effect
	NRE-GFP reporter	no effect	downregulation		no effect	no effect	no effect	no effect	no effect
EGF PATHWAY		**w1118**	**EGFR-IR**		**IFT121-IR**	**IFT122-IR**	**IFT140-IR**	**IFT43-IR**	**IFT144-IR**
ap>	Aos-lacZ reporter	no effect	downregulation		no effect	no effect	no effect	no effect	no effect

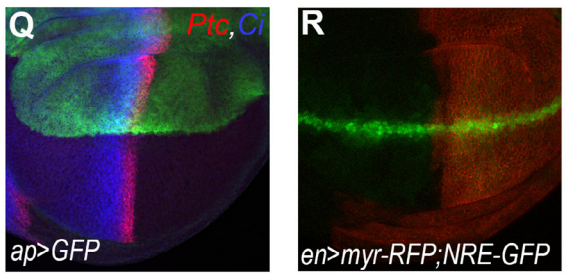

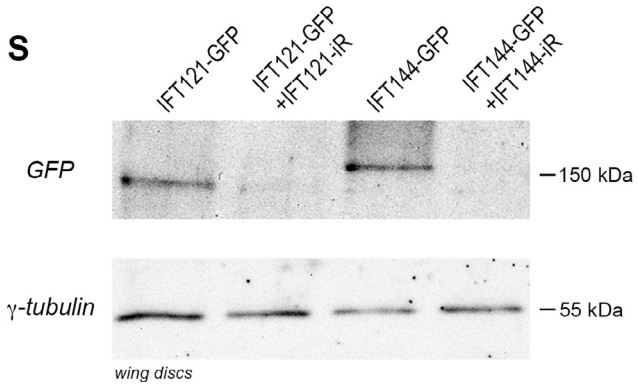

IFT-A phenotypes in adult flies, and measure of RNAi efficiency.

(**A-J**) Adult wing phenotypes induced by IFT-A component knockdowns via RNAi (IR) (n=30 per genotype). Percentages in upper right corner correspond to the percentage of flies observed with phenotype different from *wt* control wings in each experiment.

(**A-E**) *en*-driven *IFT122*-IR (**A**), *IFT140*-IR (**B**), *IFT121*-IR (**C**) and *IFT43*-IR (**D**) induce margin defects, as exemplified by notches and/or loss of wing margin bristles (black arrowheads) and weak growth and vein defects, *IFT144*-IR (**E**) resembles *wt* (100%). (**F-J**) *nub*-driven *IFT122*-IR (**F**) displays growth defects and *IFT140*-IR (**G**), *IFT121*-IR (**H**), and *IFT43*-IR (**I**) knockdowns show notches (black arrowheads) and growth defects, *nub>IFT144*-IR again resembles *wt* (**J**). (**K-O**) The respective IFT-A knockdowns in the thorax using *apGal4* resemble wild-type.

(**P**) Summary table of the different molecular target genes tested for the respective developmental signaling pathway, as indicated on left. In addition to testing Ptc and Wg staining in the secondary screen, IFT-A KD showed no effect on Ci (Hh signaling) and *NRE-GFP* (Notch signaling), compared to the controls. (**Q**) Wt expression patterns of Ci and Ptc and (**R**) *NRE-GFP.*

(**S**) Western Blot of 3rd instar wing disc lysates of IFT121-GFP and IFT144-GFP in a *wt* background, and the respective RNAi conditions as indicated showing specific silencing of each RNAi line for the respective IFT-A component (n=50 wing discs/genotype, experiment was repeated twice with the same result). *nub-Gal4* was used to express the GFP-tagged IFT-A proteins throughout wing discs, either alone or in combination with the respective RNAi construct (as indicated), and changes in protein levels were monitored. RNAi targeting of both genes reduced their protein expression to barely detectable levels, indicating that IFT144 is efficiently silenced.

Figure S3, related to Figure 3.

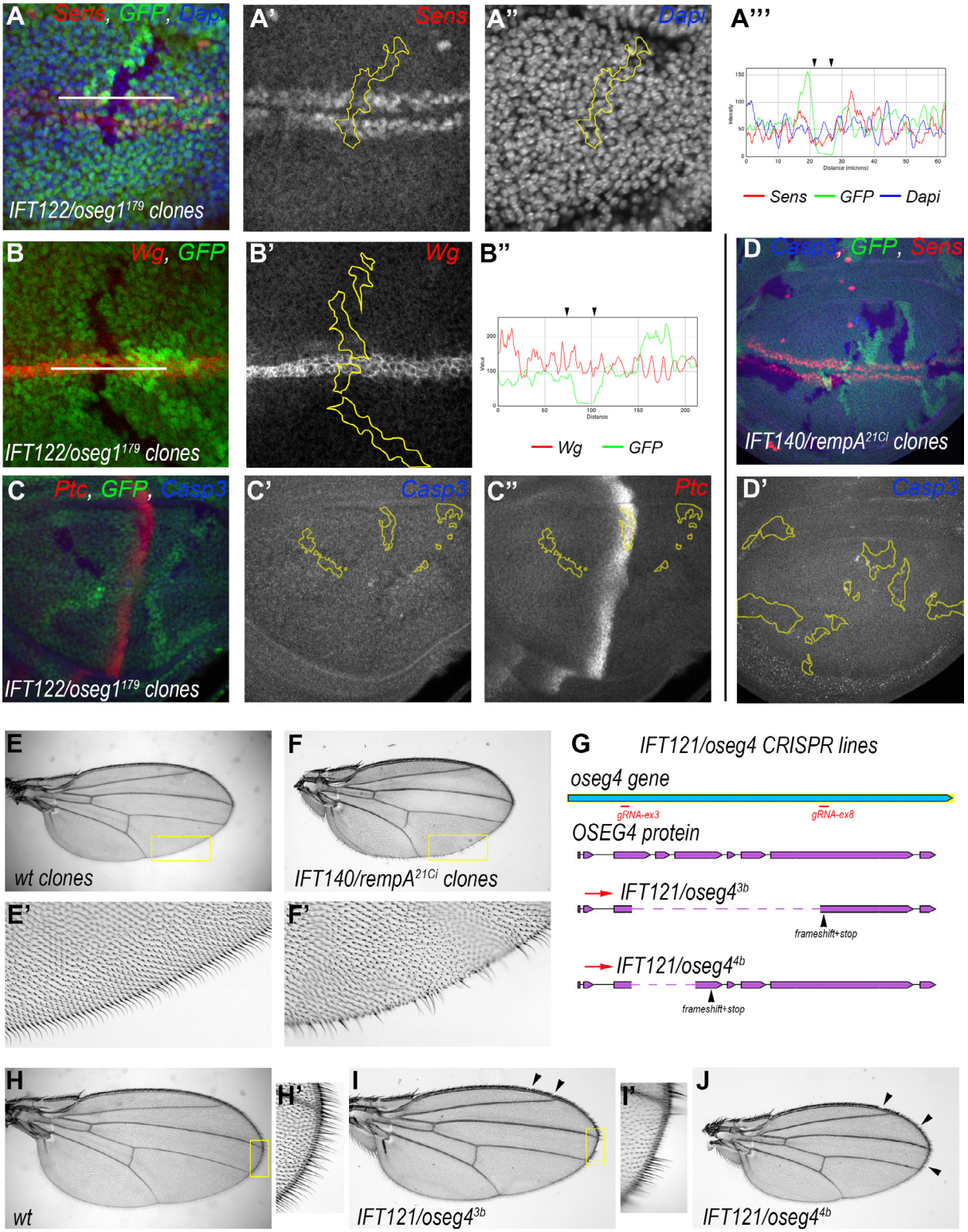

Analyses of homozygous clones of IFT-A mutants.

(A-B) Expression of Wg signaling targets Sens and Dll is reduced in *IFT122/oseg1*^{179} mutant cells, whereas expression of the Notch target Wg remains unaffected. (**A**) *IFT122/oseg1*^{179} cells (marked by absence of GFP) display reduced levels of nuclear Sens (red, monochrome in **A'**; nuclei are counterstained with Dapi: blue, monochrome in **A"**). Quantification line profiling in **A"'** (line profile/image field as indicated in **A**). (**B-C**) Other signaling pathways are not disrupted by loss of *IFT122*. (**B**) Notch signaling is unaffected in *IFT122/oseg1*^{179} (marked by absence of GFP). (**B"**) Line scan of Wg staining, note that Wg expression is not affected within the *IFT122* mutant cells (borders of mutant clone are indicated by black arrowheads above line scan; note loss of GFP in area between arrowheads). (**C**) Hedgehog pathway activity, as indicated by Ptc expression (red in **C**, monochrome in **C''**, note mutant clone within the Ptc expression domain), remains unchanged in IFT122 mutant cells. (**C-D'**) Cleaved Casp3 staining (blue in **C** and **D**; monochrome in **C'** and **D'**) in *IFT122* and *IFT140* mutant cells, respectively (genotypes and other labels as indicated). Panel **D** shows same wing area as in **Fig. 3C** in main text. Cleaved Caspase3 staining is occasionally detected in cells at the borders of mutant clones, similar to observations in Wg pathway mutant clones (see main text for reference to previous Wg-signaling studies).

(**E-F**) *IFT140/rempA*^{21Ci} clones (**F-F'**) in adult wings show disruption of the margin bristle pattern, compared to the control wing (**E-E'**), yellow rectangles in **E** and **F** indicate higher magnification field of the wing margin shown in **E'** and **F'**.

(**G**) Schematic representation of the strategy and sequence analysis of CRISPR generated *IFT121/oseg4* mutant lines. Allele/line 3b contains a deletion of exon 3 to exon 8 and insertion of few nucleotides at the breakpoint during DNA repair induced a frameshift and early stop codon in exon 8. Mutant allele/line 4b contains a deletion of exon 3 to exon 5 and insertion of few nucleotides at the breakpoint during DNA repair induced a frameshift and early stop codon in exon 5.

(**H-J**) *IFT121/oseg4*^{3b} (**I**) and *IFT121/oseg4*^{4b} (**J**) homozygous adult flies show mild disruptions at the wing margin (black arrowheads), compared to *wt* wing (**H**), yellow rectangles indicate higher magnification fields shown in **H'** and **I'**.

Figure S4, related to Figure 4.

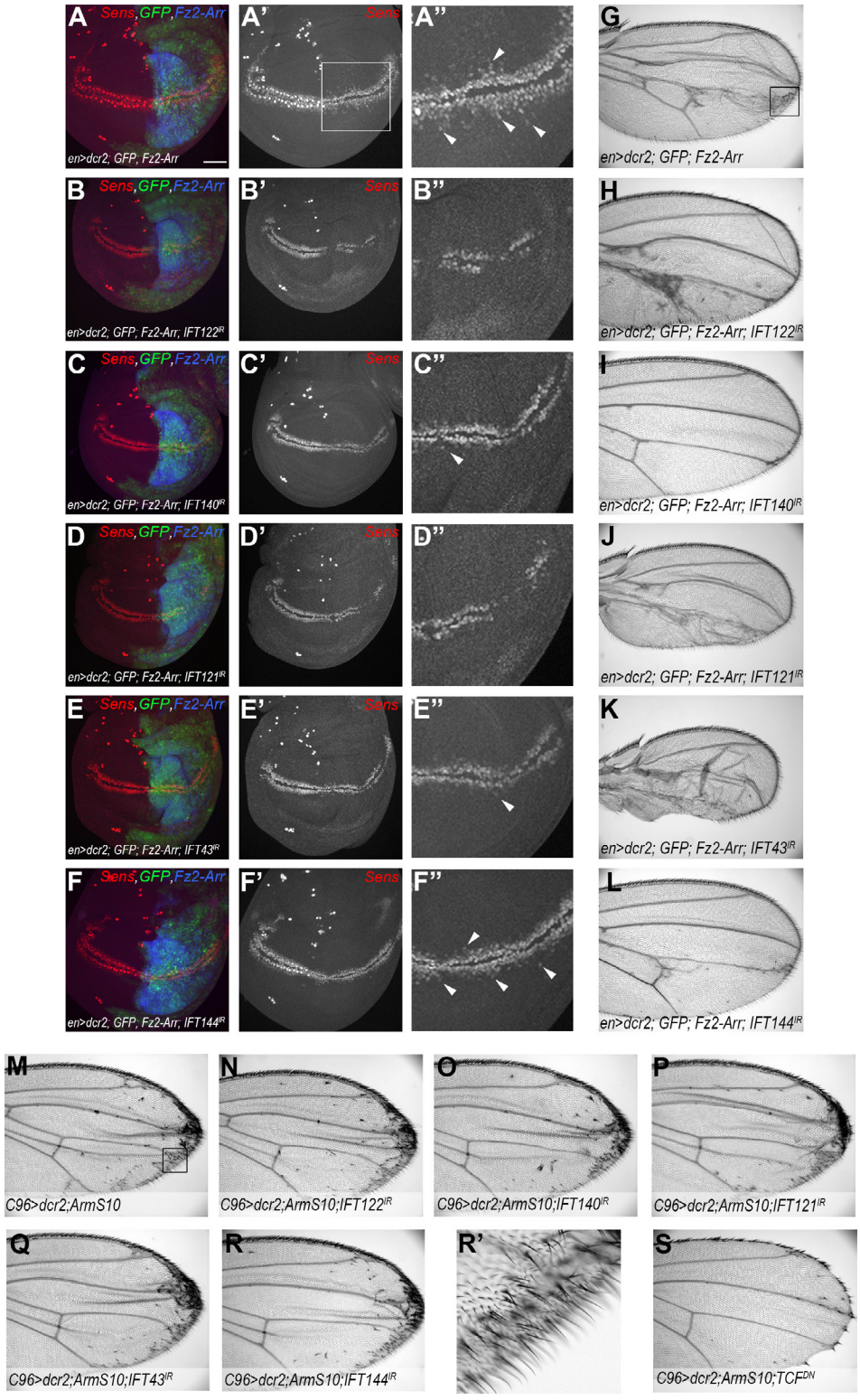

***In vivo* epistasis experiments.**

(**A-L**) Co-expression of UAS-Fz2-Arr and IFT-A RNAis using *enGal4* in 3rd instar wing discs and adult wings.

(**A**) Extra Sens positive cells (red, monochrome in **A', A"**) are observed in the posterior compartment of *en>Fz2-Arr-myc* expressing 3rd instar wing discs (examples indicated with white arrowheads), GFP (green) and Fz-Arr (blue, marked with anti-myc) expression indicate the posterior compartment. White square (**A'**) delimits the area shown at high magnification in **A"**. (**B-F**) The induction of extra Sens positive cells is suppressed by *IFT122-IR* (**B-B"**), *IFT140-IR* (**C-C"**), *IFT121-IR* (**D-D"**) and *IFT43-IR* (**E-E"**) knockdowns, but not by *IFT144-IR* (**F-F"**) (n≥20 per genotype). (**G**) In adult wings, the induction of extra Sens positive cells is reflected by the formation of extra margin bristles on the wing blade in the posterior compartment of Fz2-Arr expressing flies, black square indicates the areas shown at high magnification in main text **Figure 4A-F**.

(**H-L**) Formation of extra bristles is suppressed by the RNAi-based silencing of IFT122 (**H**), IFT140 (**I**), IFT121 (**J**), and IFT43 (**K**), but not IFT144 (**L**), correlating with Sens staining in larval wing discs. Note the resemblance between the morphology of the posterior compartment in IFT-A RNAi alone (Figure **S2A-D**) or in combination with Fz2-Arr (**H-K**), indicating that IFT-A components act downstream of the receptor complex. Quantification of the extra bristle phenotype is shown in main text **Figure 4G**.

(**M-S**) Adult wing images of *C96>ArmS10* alone (**M**; box indicates area used for quantification and shown at higher magnification in main text **Figure 4H-M**) or together with KD of *IFT-122* (**N**), *IFT140* (**O**), *IFT121* (**P**), *IFT43* (**Q**), *IFT144* (**R,** shown at high magnification in **R'**), and TCF^{DN} (**S**). IFT-A KDs do not suppress the extra-bristle phenotype induced by the expression of ArmS10, whereas TCF^{DN} does.

Figure S5, related to Figure 5.

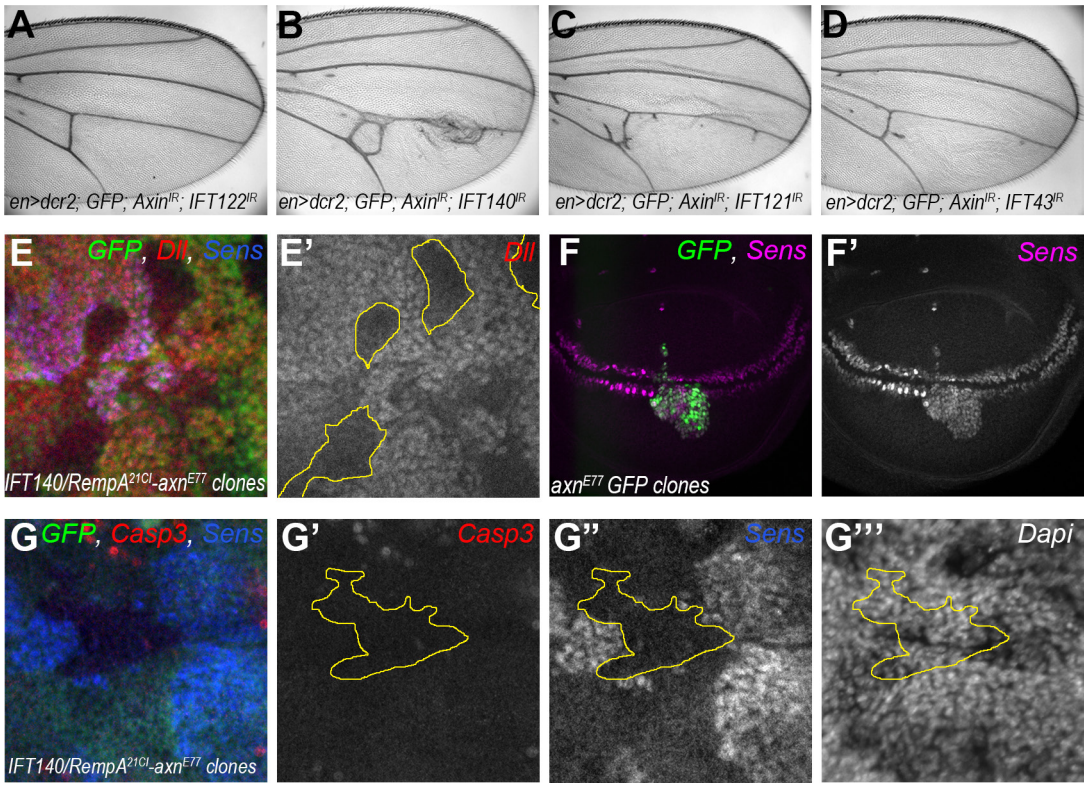

Rescue of adult viability of Axin KD flies by IFT-A KD and Axn^{E77} MARCM clones.

(**A-D**) *Axin*-IR adult viability is rescued to almost *wt* when co-expressed with *IFT122*-IR (**A**), *IFT140*-IR (**B**), *IFT121*-IR (**C**), and *IFT43*-IR (**D**)(all expressed under *en-Gal4* control).

(**E-E'**) Overactivation of Dll expression (red, monochrome in **E'**) is rescued in *IFT140/rempA^{21Ci}, axn^{E77}* double mutant clones (marked by absence of GFP; similarly to Sens (**Fig. 5H"**)), when compared to *axn^{E77}* single mutant clones. Note that only double mutant clones lack GFP, single mutant *axn^{E77}* clones show increased Dll expression, while single mutant *IFT140/rempA^{21Ci}* clones show reduced Dll levels.

(**F-F'**) *axn^{E77}* MARCM clones (marked by GFP expression) display overactivation of Sens (magenta, monochrome in **F'**).

(**G-G'"**) Cleaved-Caspase3 staining (red, monochrome in **G'**) and Sens staining (blue, monochrome in **G"**) in *IFT140/rempA^{21Ci}, axn^{E77}* double mutant clones; note that Sens overactivation is suppressed in cells of the double mutant clone (outlined with yellow line in **G'-G'"**; Dapi stains all nuclei in **G'"**).

Figure S6, related to Figure 6

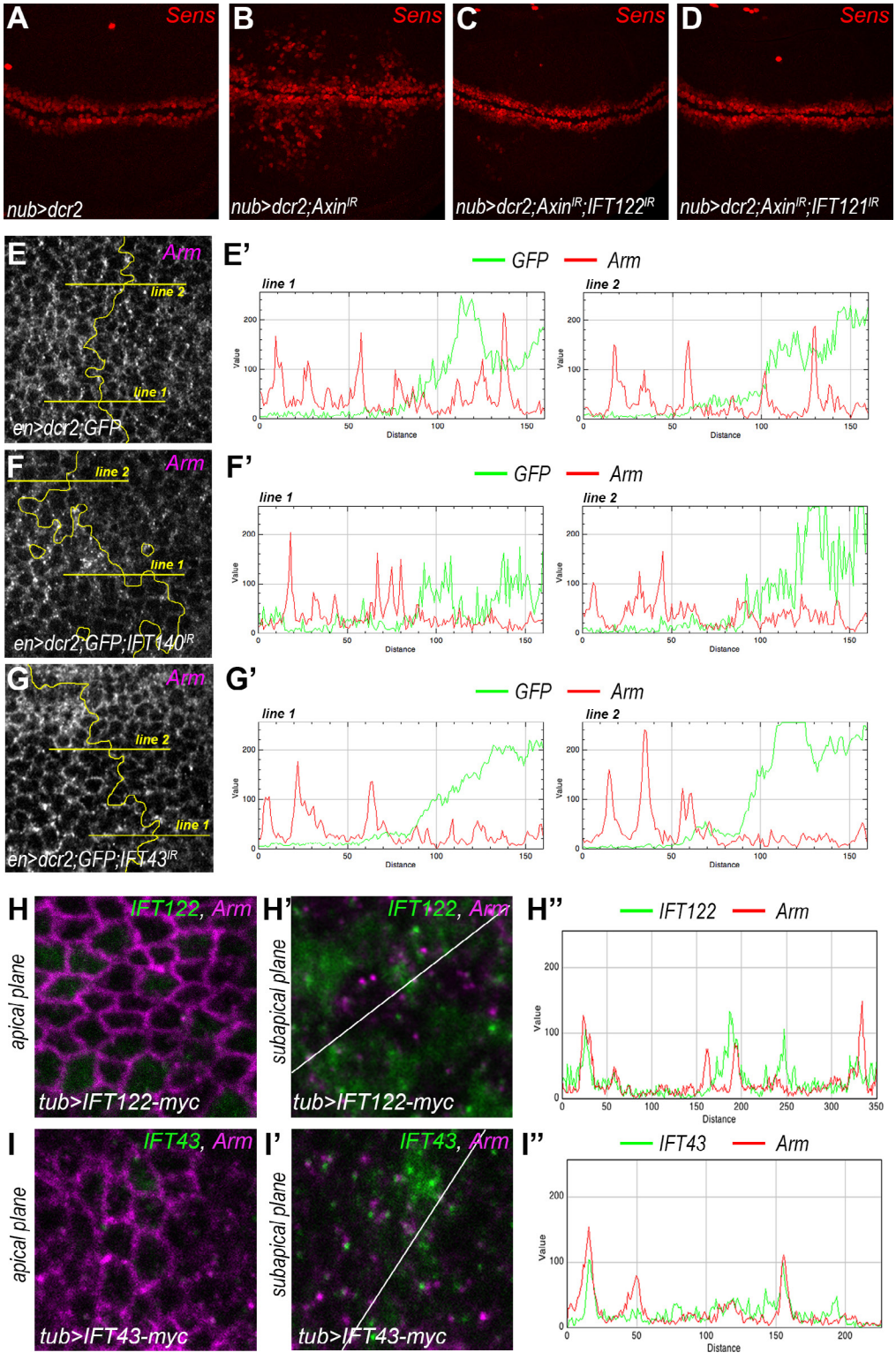

Line scan quantification of cytoplasmic Arm levels in IFT-A KD and colocalization plots of IFT-A and Arm

(**A**) Wt pattern of Sens (red) in flies expressing *nub>dcr2*. (**B**) Ectopic Sens positive cells are induced by *nub*-driven *Axin*-IR mediated KD, compared to *wt* in **A** (note that the effect is milder than with *en-Gal4* (main text **Fig. 5A**) and Sens is not activated in all cells of the wing pouch expressing *nub*. (**C-D**). Suppression of ectopic Sens positive cell phenotype in *nub*-driven *Axin*-IR KD with co-expression of RNAi to *IFT122* (**C**) or *IFT121* (**D**).

(**E-G**) Quantification of cytoplasmic Arm levels. Confocal images in **E-G** are the same as in the main text **Fig. 6C'-E'**. Yellow lines indicate the line scan plotted in **E'-G'**. Note that peaks of cytoplasmic Arm are reduced in posterior GFP-positive regions (respectively IFT140 KD in **F'** and IFT43 KD in **G'**) compared to the anterior GFP-negative region and to the *wt* control in **E'**.

(**H-I**) Confocal scans of apical and subapical planes of *tub*-driven expression of IFT122-myc (**H-H'**) and IFT43-myc (**I-I'**) (green) and Arm (magenta; note that Arm staining labels the junctions in the apical planes and shows a punctate distribution in subapical areas, wing disc areas are the same as shown in main text **Fig. 6H-I**). White line indicates region/line shown in line plot of fluorescence intensity in **H"** and **I"**, note that several peaks of Arm and IFT-A-myc staining are superimposed, indicating that both proteins can colocalize.

Table S1, related to Table 1.

Adult phenotypes observed for each RNAi knockdown in the primary screen.

Vertebrate gene name	Drosophila ortholog	RNAi line #	Phenotypic classes		Additional RNAi line #
			WING	THORAX	
BBS1	CG14825, BBS1	v109623	wt	wt	NA
BBS3, ARL6	CG7735	v104462	growth, notch, vein	wt	*v43508*
BBS4	CG13232, BBS4	v100571	growth, notch, mch	wt	**v28772**
BBS5	CG1126	v18200	growth	loss	NA
BBS8	CG13691, BBS8	v32058	wt	wt	NA
BBS9	CG15666	v40013	growth (notch)	wt	**v110798**
MKS1	CG15730	v19582	wt	wt	**v19583**
MKS3	CG15923	v37373;MS54	growth, vein, mch	excess	***v107011***
TCTN1/2/3	CG42731, tectonic	v107952	wt	other	NA
B9D1	CG14870	v107330	growth	other	**v46307**
B9D2	CG42730	v40858	wt	wt	NA
NPHP6,CEP290	CG13889	NA			
NPHP9, NEK8	CG10951, niki	v100823	wt	wt	**v16120**
CC2D2A, CEP76	CG18631	v100302	vein	Lethal	*v47215*
IFT20	CG30441	v106811	wt	wt	**v50583**
IFT46	CG15161	d15161R-1	Growth	wt	**v25198**
IFT52	CG9595, osm-6	v24068	wt	wt	NA
IFT54	CG3259	v46163	Growth, vein	(loss)	NA
IFT57	CG8853, che-13	v106927	wt	wt	**v51323**
IFT70, FLEER	CG5142	v22015	growth, vein, mch	(misoriented, loss)	*v110166*
IFT80	CG9333, Oseg5	v100020	growth, vein, notch	loss	***v52551***
IFT88	CG12548, nompB	v104419	wt	lethal	**tJF00380**
IFT172	CG13809, osm-1	v107157	growth, vein, notch, mch	(loss)	***v24795***
KIF3A	CG10642, Klp64D	v103358	wt	lethal	**v45373**
KIF3B	CG7293, Klp68D	tJF03346	growth, vein (notch)	(misoriented)	***v101058***
KIF17	CG17461, Kif3C	v43641	wt	wt	NA
KIFAP3	CG11759, Kap3	v103548	vein (notch)	wt	***v45400***
IFT121, WDR35	CG2069, oseg4	v109805	Vein, notch	(misoriented)	***v43380***
IFT122	CG7161, oseg1	v103598	growth, vein	wt	***d7161R-1***
IFT140	CG11838, rempA	v31575	growth (notch)	wt	***v103424***
IFT144, WDR19	CG11237, oseg6	v38462	wt	wt	***tGLC01452***
IFT43	CG5780	v106366	growth, vein, notch	wt	NA
DYNCH2H1	CG15148, btv	tJF03010	Growth, vein	misoriented	***v105152***
DYNC2LI1	CG3769	v40469	blister	wt	**v109621**
DYNLL1	CG6998, ctp	v109084	growth (notch)	misoriented, loss (other)	**v43116**
ARL13B	CG11356	v33812	notch	wt	NA
PKD2	CG6504, pkd2	v110681	wt	wt	**tJF01468**
OFD1	CG1501, unc	tJF03403	growth	wt	NA
TULP3	CG9398, king-tubby	v29110	vein	wt	NA
CCDC104	CG14367	v100799	notch	(loss)	NA
EFHC1	CG11048, Efch1.2	v106676	wt	wt	**v31407**
CLUAP1	CG17599	v14682	growth	loss, misoriented	*d17599R-1*
TTC26	CG4525	v107708	vein	misoriented	**d4525R-2**
CEP164	CG9170	v108727	wt	wt	**v29066**
EB1	CG3265, Eb1	v24451	vein	misoriented, loss	***tHM05093***
IMPORTIN β	CG2637, Fs(2)ket	v107622	Lethal	Lethal	***tJF01755***
RFX	CG6312, rfx	v10416	growth, mch	wt	*tJF02518*
Pericentrin	CG33957, cp309	v100969	growth	misoriented	***v101645***
SAS-6	CG15524, sas-6	v25073	vein	loss	**v110149**
ROOTLETIN	CG6129, rootletin	d6129R-1	growth, vein	loss, other	*v110171*
ARL3	CG6560, dnd	v104311	growth, vein, mch, notch	loss, misoriented	**tJF02638**
RAB8	CG8287, rab8	v28092	wt	wt	***tJF02669***

LRCC16A	CG1399	[v]24826	wt	wt	NA
OSCP1	CG13178	[v]110148	wt	(misoriented, loss)	***[v]44816***
CEP192	CG17286, spd-2	[v]36623	vein	wt	*[v]101882*
CEP152	CG2919, asl	[v]25457	wt	(loss)	***[t]HMS01463***
γ-TUBULIN	CG17566, γ-Tub37C	[v]109921	wt	wt	***[t]HMS00517***
SAK/PLK4	CG7186, Sak	[v]105102	(vein)	wt	***[v]27904***
SAS-4	CG10061, sas-4	[v]106051	growth (notch)	(misoriented, loss)	***[t]HMS01463***
CP110	CG14617, cp110	[v]101161	notch	other	*[v]24874*
CENTRIN	CG17493	[v]40080	wt	wt	NA
CEP135	CG17081, cep135	[v]14194	wt	loss	NA
TEKT1	CG10541, tektin-C	[v]100094	lethal	lethal	**[v]31253**
Developmental pathway specific controls					
	Frizzled/Frizzled2	[v]43075;[t]JF01259	growth, notch, mch	misoriented	
	Notch	[v]27228	growth, notch, vein	loss/excess	
	Smoothened	[t]JF02363	growth, vein	wt	
	EGFR	[t]JF01368	growth, vein	other	
	Thickvein	[t]JF01486	growth, vein	wt	

Cilia-associated genes not considered in our study as their degree of conservation was not determined by standard sequence alignments using NCBI protein blast					
BBS2	BBS6	BBS7	BBS10	BBS11	BBS12
NPHP1	NPHP3	NPHP4	NPHP5	NPHP7, GLIS2	NPHP8, RPGRIP1L
AHI1	IFT22	IFT25/HSBP11	IFT27	IFT71/72/74	IFT81
IFT139	WDR34	PKD1	PKHD1	OFD2	ALSM1
STIL	PCM-1	FAPP2	δ-TUBULIN	CENTROBIN	KIF24

Cilia-associated genes with known functions in developmental pathways (vertebrate gene / Drosophila ortholog)		
NPHP2, INVERSIN / CG12342, Dgo	FUZ / CG13396, Fuzzy	aPKC / CG10261, aPKC
KIF7 / CG1708, Costal-2	PAR3 / CG5055, Bazooka	CRB3 / CG6383, Crumbs
INTU / CG16993, Inturned	PAR6 / CG5884, PAR6	GSK3β / CG2621, Shaggy

Bold+Italic confirmed with independent RNAi line, **Bold** confirmed with overlapping RNAi line, *Italic* not confirmed by 2nd RNAi line, NA: not available, ( ) penetrance less than 50%, mch stands for multiple cellular hairs, [v] vdrc collection, [d] dgrc kyoto collection, [t] trip collection, [MS] made in our lab

Experimental procedures

Antibodies

For tissue staining, primary antibodies include guinea pig anti-Senseless (1:500, gift from H. Bellen), mouse anti-Wingless (1:500, DSHB 4D4 concentrate), mouse anti-Armadillo (1:10, DSHB 7A1), rat anti-DE-cad (DSHB DCAD2), rat anti-Distalless (1:250, (Wu and Cohen, 2000), mouse anti-myc (1:200, Santa Cruz, 9E10), rabbit anti-myc (1:200, Santa Cruz, d1-717), mouse anti-Ptc (1:50, DSHB 5E10), rat anti-Ci (1:500, DSHB 2A1 concentrate), rabbit anti-beta-galactosidase (1:500, Molecular Probes A11132), mouse anti-acetylated tubulin (1:2, gift from C. Iomini). For immunoblotting, the following primary antibodies were used: mouse anti-Armadillo (1:1000, DSHB 7A1), mouse anti-γ-tubulin (1:1000, Sigma), mouse anti-GFP (1:1000, Roche), rabbit anti-cleaved Caspase-3 (D175, Cell Signaling). Fluorescent secondary antibodies and HRP-coupled secondary antibodies were from Jackson Laboratories.

Transgenic flies and plasmids pUASt-IFT122-myc and pUASt-IFT43-myc

To generate UAS-IFT122-myc transgenic flies, Myc tag was added to the C-term of IFT122 sequence by PCR amplification using DGRC SD05642 cDNA clone and cloned into pUASt vector using NotI and XbaI sites. The following primers were used: 5'-GCGGCCGCTATGAGGGGTGTTCTCAAGTGG-3' and 5'-GCTCTAGACTACAGATCTTCTTCAGAAATAAGTTTTTGTTCAAAGTCTTCCATCAGCTTTTCGG-3'.

To generate UAS-IFT43-myc transgenic flies, Myc tag was added to the C-term of IFT43-myc sequence by PCR amplification using DGRC SD05240 cDNA clone and cloned into pUASt vector using NotI and XbaI sites. The following primers were used: 5'-GCGGCCGCTATGGACTGGGCCGAAGAAC-3' and 5'-GCTCTAGACTACAGATCTTCTTCAGAAATAAGTTTTTGTTCAGTATATTGTGTGGGTGGAATC-3'.

CRISPR mutant oseg4

We used the protocols from (Kondo and Ueda, 2013) to construct a double-gRNA vector. The primers used to insert gRNA into pBFv-U6.2B were: U6.2-oseg4-ex3-1F 5'-CTTCGTACAGATGACACTCCCCGT-3', U6.2-oseg4-ex3-1R 5'-AAACACGGGGAGTGTCATCTGTAC-3', U6.2B-oseg4-ex8-1F 5'-CTTCGCGGAGATATCAGCCTTCTA-3' and U6.2B-oseg4-ex8-1R 5'-AAACTAGAAGGCTGATATCTCCGC-3'. This construct was then injected in the TBX-0002 *y^1 v^1 P{nos-phiC31\int.NLS}X; attP40* fly stock and crossed with CAS-0002 *y^2 cho^2 v^1 P{nos-Cas9, y+, v+}1A/FM7c, KrGAL4 UAS-GFP* for generation of CRISPR mutant. Mutants were selected by non lethal genotyping (Carvalho et al., 2009) and amplification of the targeted region by PCR.

References

Carvalho, G.B., Ja, W.W., and Benzer, S. (2009). Non-lethal PCR genotyping of single Drosophila. BioTechniques *46*, 312–314.

Kondo, S., and Ueda, R. (2013). Highly improved gene targeting by germline-specific Cas9 expression in Drosophila. Genetics *195*, 715–721.

Wu, J., and Cohen, S.M. (2000). Proximal distal axis formation in the Drosophila leg: distinct functions of teashirt and homothorax in the proximal leg. Mechanisms of Development *94*, 47–56.